Appl. Phys. B (2005)
DOI: 10.1007/s00340-005-2062-4

Applied Physics B
Lasers and Optics

A.M. ZHELTIKOV[1,✉]
M.N. SHNEIDER[2]
R.B. MILES[2]

Radar return enhanced by a grating of species-selective multiphoton ionization as a probe for trace impurities in the atmosphere

[1] Physics Department, International Laser Center, M.V. Lomonosov Moscow State University, Moscow 119992, Russia
[2] Department of Mechanical and Aerospace Engineering, Princeton University, Princeton, NJ 08544-5263, USA

Received: 5 October 2005

ABSTRACT Two-color time-ordered dyads of short laser pulses induce a spatially periodic modulation of the refractive index of the atmosphere through resonance-enhanced multiphoton ionization (REMPI), enhancing the back reflection of radio waves. The carrier frequencies and the timing of laser pulses in a dyad provide a unique code for selectively accessing the manifold of energy levels of impurity molecules, inducing REMPI gratings of the refractive index only in the presence of impurity molecules, thus suggesting an attractive strategy for the radar-based stand-off detection of trace impurities in the atmosphere.

PACS 42.70.Qs; 42.65.Wi

1 Introduction

Remote sensing of low concentrations of impurity molecules in the atmosphere has always been considered as one of the most important problems in applied science. Recent terrorist attacks and ever-growing threats of using chemical and bacteriological agents put the problem of remote sensing in the context of national security, making it one of the strategic issues for the protection of the civilian population in the war of nations against terror. Light detection and ranging (LIDAR) [1] is a powerful technique for the remote sensing of trace impurities in the atmosphere. LIDAR capabilities have been recently substantially enhanced through the use of high-intensity ultra-short laser pulses [2], which can propagate over large distances in the atmosphere in the regime of filamentation [3, 4], providing valuable information on the contamination level of atmospheric air [5]. Another promising approach to the stand-off detection of trace impurities in the atmosphere, as shown by recent theoretical studies [6, 7], can be based on coherent anti-Stokes Raman scattering (CARS) and superradiance phenomena combined with the methods of ultra-fast nonlinear spectroscopy [8] using adaptively shaped ultra-short pulses [9] and coherence-controlled population transfer [10–12].

In this work, we show that species-selective resonance-enhanced multiphoton ionization (REMPI), induced by two-color time-ordered dyads of short laser pulses and detected by back-reflected radio waves, offers an attractive strategy for the radar-based stand-off detection of trace impurities in the atmosphere. The carrier frequencies and the timing of laser pulses in a dyad provide a unique code for selectively accessing the manifold of energy levels of impurity molecules, inducing REMPI-seeded ionization only in the presence of impurity molecules. Chirped trains of such pulse dyads can then induce a grating of the refractive index through the REMPI-seeded ionization process, radically increasing the return of probing radar radiation and improving the sensitivity of stand-off impurity detection. The approach proposed here is thus based on a species-selective REMPI of trace impurities in the atmosphere using optimized sequences of laser pulses (Fig. 1). Time separations between the pulses in the sequence are chosen in such a way as to induce a periodic modulation of the refractive index of the gas through species-selective REMPI in order to enhance the return of radio waves and improve the sensitivity of radar detection of impurities in the atmosphere. In what follows, we consider in greater detail all the ingredients of this approach.

2 Species-selective resonance-enhanced multiphoton ionization of impurities

We start with the REMPI process, which is used in our approach for a selective ionization of impurity molecules, providing a change in the refractive index of the gas. As a generic example of two-color species-selective REMPI, we consider a sequential ionization of OClO molecules by UV pump pulses and a time-delayed visible probe field, experimentally demonstrated by Zewail's group [13]. As shown in Fig. 2, a UV pulse with a central wavelength of 329 nm serves to excite a group of vibrational levels in the $A\,^2A_2$ excited state of OClO through a one-photon transition from the $X\,^2B_1$ ground state of this molecule. The probe pulse with a central wavelength of 620 nm then ionizes excited-state OClO molecules through a four-photon transition from the $A\,^2A_2$ state.

Multiphoton ionization of OClO by the UV pump field alone, which would create an unwanted background in our arrangement, can be readily minimized by the adjustment of the intensities of the pump and probe pulses. In experiments [13],

✉ Fax: +7-095-939-5174, E-mail: zheltikov@top.phys.msu.su

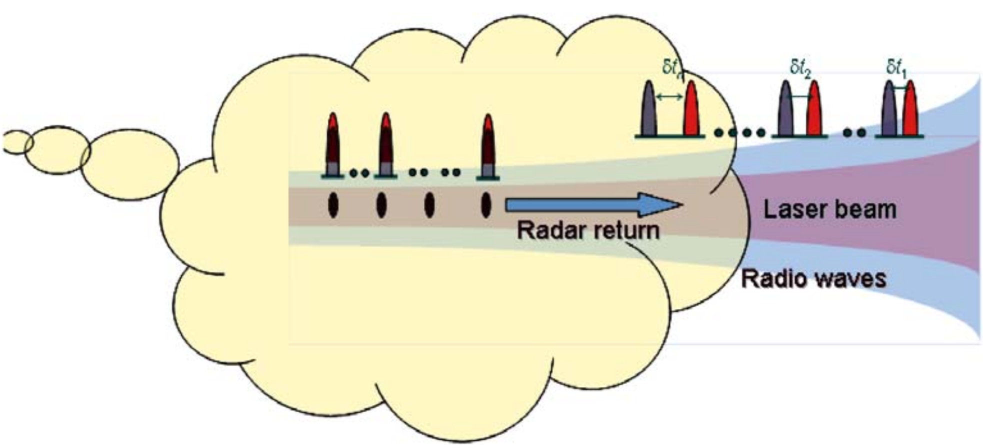

FIGURE 1 Radar return enhanced by a REMPI grating. Two-color time-ordered dyads of short laser pulses induce a spatially periodic modulation of the refractive index of the atmosphere through resonance-enhanced multiphoton ionization, enhancing the back reflection of radio waves

the time-independent background due to the multiphoton ionization of OClO molecules by the pump field alone was less than 10% with respect to the two-color REMPI signal. The ionization process under these conditions is confined to the area where the pump and probe pulses overlap in time and space.

A further improvement in the ratio of the two-color REMPI signal to the background related to ionization induced by the pump pulse alone can be expected for molecular systems where a nonzero time delay between the pump and probe pulses would allow a vibrational wave packet excited by the pump field to evolve toward the state providing the maximum probability of multiphoton ionization in the presence of the probe field. Examples of such transitions can be found in the extensive literature on the ultra-fast pump–probe spectroscopy of wave-packet dynamics in molecular systems (see e.g. [8] for a review). In particular, as shown by elegant experiments reported by Baumert et al. [14, 15], Na_2 molecules can be ionized through a two-step time-delayed transition involving a resonant absorption of one 340-nm pump-field photon, resulting in the excitation of the $2\,^1\Sigma_u{}^+$ state, and a subsequent resonant absorption of a time-delayed 540-nm probe-field photon. The broadband pump field creates a vibrational wave packet at the inner turning point of the $2\,^1\Sigma_u{}^+$ state, which moves then in the double-minimum state of the Na_2 molecule. The central wavelength of the probe field is chosen in such a way as to maximize, according to the Franck–Condon principle, the probability of transition into the repulsive $^2\Sigma_u{}^+$ state at the outer turning point of the $2\,^1\Sigma_u{}^+$ state. As shown by Baumert et al. [14, 15], when the energy of the pump photon is enough to create a wave packet above the potential barrier of the double-minimum potential sensed by the system in the $2\,^1\Sigma_u{}^+$ state, the probe pulse with a wavelength of 540 nm gives rise to clean, temporally periodic peaks in the ion yield. According to the experimental data [14, 15], the Na^+ yield measured for the optimal delay time between the probe and pump pulses is about five times higher than the ion yield corresponding to negative delay times, i.e. probe pulses applied before the pump field. Other possible strategies to improve the selectivity of the REMPI process with respect to the sort of species can employ the methods of phase control of quantum transitions in molecular systems using adaptively shaped pulses or optimized time-ordered pulse sequences [10–12].

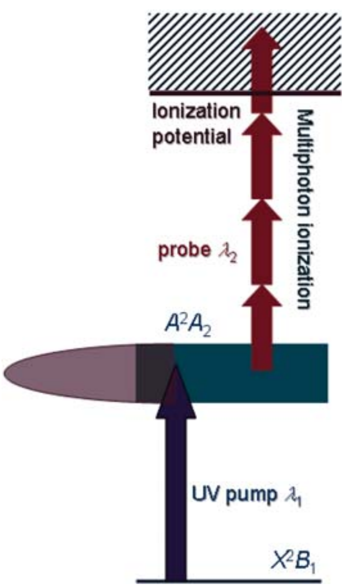

FIGURE 2 A simplified diagram of two-color REMPI of OClO (after Baumert et al. [13]). A broadband femtosecond pulse serves to excite a group of vibrational levels in the $A\,^2A_2$ excited state of OClO through a one-photon transition from the $X\,^2B_1$ ground state of this molecule. The probe femtosecond pulse ionizes excited-state OClO molecules through a four-photon transition from the $A\,^2A_2$ state

3 Optimal pulse sequences

In this section, we will show that optimized sequences of ultra-short laser pulses can induce a spatially periodic modulation of the electron number density through the REMPI process. This modulation creates a grating of the refractive index in remote objects in the atmosphere, enhancing the back reflection of radio waves (Fig. 1). To accomplish this plan, we consider a sequence of pulse dyads similar to that proposed earlier by Kocharovsky et al. [7] for the stand-off superradiant detection of trace impurities in the atmosphere. The delay time δt_i between the laser pulses in the nth dyad of our sequence is designed in such a way (Fig. 1) as to make the pulses overlap in space and time at a certain distance z_i in the atmosphere. The sequence of pulse dyads is chirped, i.e. the pulse separation δt_i is changed from dyad to dyad so that $z_{i+1} - z_i = \delta z$, thus providing a REMPI-induced periodic modulation of the refractive index of the gas with a spacing δz.

We set the wavelengths of the pump and probe pulses equal to $\lambda_1 = 330$ and $\lambda_2 = 620$ nm, corresponding to a two-color REMPI of OClO molecules, as shown in Fig. 2. To include the influence of group-delay and temporal stretching effects on the propagation of these pulses, we use the Cauchy formula to calculate the dispersion of the atmospheric-pressure air. We represent the group index of the atmospheric air at the wavelength λ as $n_g(\lambda) \approx 1 + \delta n(\lambda)$, where $\delta n(\lambda)$ is the small addition shown by the solid curve in Fig. 3. The group-velocity mismatch of 620- and 330-nm pulses is then estimated as $\Delta v = v(\lambda_2) - v(\lambda_1) \approx c[\delta n(\lambda_1) - \delta n(\lambda_2)] \approx 1.2 \times 10^6$ cm/s, where c is the speed of light in vacuum. The faster 620-nm pump pulse catches up with the slower 330-nm probe pulse at the distance of $z_1 \approx 1$ km if the probe pulse is initially delayed in time with respect to the pump pulse by an interval $\delta t_1 \approx z_1[\delta n(\lambda_1) - \delta n(\lambda_2)]/c \approx 130$ ps. To create a REMPI grating with a typical spacing of $\delta z \approx 50$ cm, the delay time between the pump and probe pulses should be increased by $\delta t = \delta t_{i+1} - \delta t_i \approx 70$ fs from dyad to dyad.

Due to its nonlinear nature, the REMPI process is strongly confined to the regions where both the pump and probe pulses have maximum intensities, with the probability of N-photon ionization following roughly (see e.g. [13]) the cross-correlation function of the pump and probe pulses, $F_c(t) \propto \exp(-Nt^2/\tau_0^2)$, where τ_0 is the pulse duration in the interaction region. Setting $N = 5$ for the $(1+4)$-REMPI process sketched in Fig. 2, we find that the pump and probe pulses with the above-specified wavelengths overlap in time and space over the characteristic length of $l \approx c\tau_0/\{\sqrt{5}[\delta n(\lambda_1) - \delta n(\lambda_2)]\} \approx 30$ cm for $\tau_0 \approx 100$ fs. Laser pulses with a temporal width τ experience pulse stretching as they propagate through a dispersive medium within a characteristic dispersion length, given by $L_d = \tau^2/|k_2|$. For 330-nm pulses propagating in the atmospheric air, $k_2 \approx 0.5$ fs^2/cm (the dashed curve in Fig. 3), giving $L_d \approx 0.2$ km for 100-fs pulses. Delivering 100-fs pulses to remote objects located at typical distances within a kilometer range in the atmosphere may therefore require dispersion pre-compensation, e.g. by initially chirping the pulses. Another solution could include an initial phase of nonlinear-optical propagation of laser pulses, involving temporal and spatial self-action phenomena, similar to those observed in experiments on filamentation of high-power laser pulses in the atmosphere [5]. As can be seen from the above expression for the pulse-overlap length l, the modulation amplitude of the REMPI grating can be increased by using pump–probe dyads with larger wavelength separations and higher-N multiphoton ionization processes.

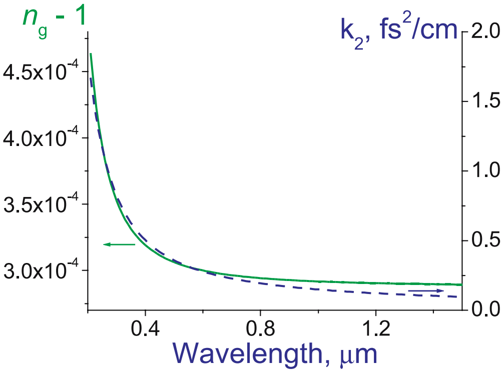

FIGURE 3 Group index and group-velocity dispersion k_2 as functions of the wavelength for atmospheric-pressure air

4 Bragg-reflected radar return

Free electrons generated as a result of the species-selective REMPI process modify the refractive index of the gas. In Fig. 4, we present the real and imaginary parts of the complex refractive index $\tilde{n} = n_p + i\kappa$ of an ionized gas calculated as a function of radiation frequency $f = \omega/2\pi$ in the radio-frequency range using standard equations of plasma physics, $2n_p^2 = \varepsilon + [\varepsilon^2 + (4\pi\sigma/\omega)^2]^{1/2}$ and $2\kappa^2 = -\varepsilon + [\varepsilon^2 + (4\pi\sigma/\omega)^2]^{1/2}$, where $\varepsilon = 1 - \omega_p^2/(\omega^2 + \nu^2)$, $\sigma = e^2 n_e \nu/[m(\nu^2 + \omega^2)]$, e is the electron charge, n_e is the electron density, ω is the radiation frequency, $\omega_p = (4\pi e^2 n_e/m)^{1/2}$ is the plasma frequency, m is the electron mass, and ν is the effective collision frequency. We are primarily interested in the case of low electron densities, when it is especially difficult to detect a small region of gas ionization. For the characteristic electron density $n_e = 10^{11}$ cm^{-3}, for example, $\kappa \approx 10^{-2}$, corresponding to a skin-layer depth of about 5 m for 1-GHz radiation. The ionization-induced change in the refractive index of the gas in this regime is very small, $n_p - 1 \approx 3 \times 10^{-5}$, leading to a low reflectivity of the ionized volume.

The return of radar radiation can be increased through the constructive interference of the waves reflected from the refractive-index grating, induced in the gas through the REMPI process by two-color time-ordered dyads of short

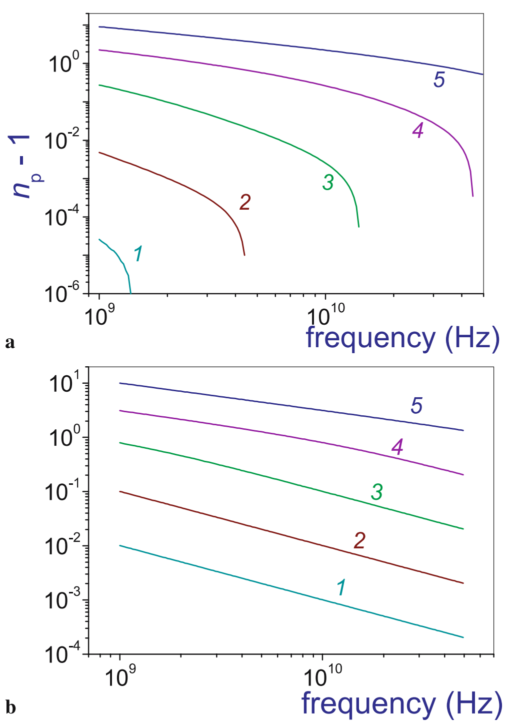

FIGURE 4 The real (**a**) and imaginary (**b**) parts of the refractive index of an ionized gas in the radio-frequency range as a function of radiation frequency. The density of electrons is (1) 10^{11} cm^{-3}, (2) 10^{12} cm^{-3}, (3) 10^{13} cm^{-3}, (4) 10^{14} cm^{-3}, and (5) 10^{15} cm^{-3}

laser pulses (Fig. 1), optimized as described in the previous sections. The maximum reflectivity of the REMPI-induced grating is achieved when the reflected wave is Bragg-resonance-coupled to the incident wave. The REMPI grating acts as a distributed Bragg reflector in this case. In the regime of normal incidence, this condition of a Bragg resonance, defining the center of the photonic band gap of a periodic structure, is written as $\bar{n}\omega/c = \pi m/d$, where $\bar{n} = [(n_1^2 + n_2^2)/2]^{1/2}$, n_1 and n_2 are the refractive indices of the materials forming the periodic structure, d is the period of the grating, and m is an odd integer. Maximum reflection is thus achieved when the grating period roughly accommodates an odd integer number of half-wavelengths. The coefficient of reflection of such a grating with $n_1 \approx n_2 \approx 1$ and $|n_1 - n_2| = \delta n$ is given by [15] $R \approx \tanh^2(\sqrt{2}\delta n N d/\lambda)$, where N is the number of periods in the grating.

Figure 5 displays the reflection coefficient R for the REMPI-induced grating with $\delta n = n_\text{p} - 1$ calculated as a function of the frequency of the radar signal for different δn. For small values of the argument $x = \sqrt{2}\delta n N d/\lambda$, the Taylor-series expansion of the expression for the reflection coefficient gives $R \approx 2(\delta n)^2 N^2 (d/\lambda)^2$. The N^2 dependence of the reflection coefficient on the number of periods (curves 1–3 in Fig. 5) indicates that the contributions from individual layers forming the REMPI grating add up coherently, enhancing the return of the radio-wave probe radiation. An order-of-magnitude enhancement of the back-reflected signal can thus be achieved by increasing N by a factor of three.

In the regime $x \ll 1$, the reflection coefficient R tends to unity (curve 4 in Fig. 5). In the absence of losses, such a grating would provide a 100% reflection of the incident wave. For an ionized gas, however, large values of δn, achieved with high electron densities n_e, correspond to high losses $\kappa \approx n_\text{p} \approx (2\pi\sigma/\omega)^{1/2}$ (cf. curves 4 and 5 in Fig. 4a and b in the frequency range of 1–10 GHz). Regimes with $\approx 100\%$ reflection are therefore difficult to implement experimentally for REMPI gratings.

Two other important physical factors have to be taken into consideration for the practical implementation of the REMPI-grating-based stand-off detection technique proposed here. Firstly, for one-dimensional REMPI gratings with transverse sizes comparable to or less than the wavelength of probing radio waves, diffraction can substantially reduce the backward radar return. Optimally phased two-dimensional REMPI gratings may be necessary in this regime to shape the radar-return radiation pattern with the central maximum in the backward direction. Secondly, the coherence of radar waves tends to degrade in a turbulent atmosphere. A complementary technique, based on the Rayleigh scattering of radio waves by properly structured arrays of ionized microvolumes in the atmosphere, can then be used to improve the radar return. Recent theoretical [16] and experimental [17] studies show that such microvolumes of ionized gas can be efficiently detected by using radar microwave Rayleigh scattering. A combination of REMPI gratings and Rayleigh scattering thus suggests a promising technique for the radar-based stand-off detection of trace impurities in the atmosphere within a broad range of atmosphere parameters.

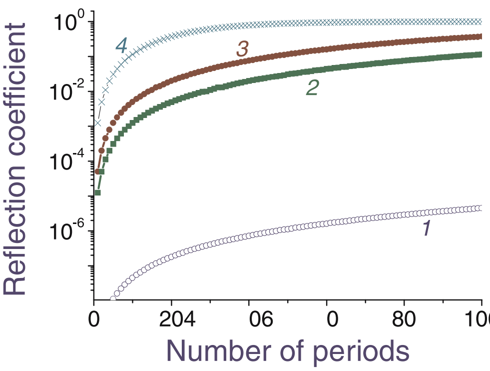

FIGURE 5 Reflection coefficient of a one-dimensional periodic structure with a refractive-index step $\Delta n = 3 \times 10^{-5}$ (1), 5×10^{-3} (2), 10^{-2} (3), and 5×10^{-2} (4) as a function of the number of periods N

5 Conclusion

We have shown in this work that species-selective resonance-enhanced multiphoton ionization, induced by two-color time-ordered dyads of short laser pulses and detected by back-reflected radio waves, can be used for the radar-based stand-off sensing of trace impurities in the atmosphere. The carrier frequencies and the timing of laser pulses in a dyad provide a unique code for selectively accessing the manifold of energy levels of impurity molecules, inducing REMPI-seeded ionization only in the presence of impurity molecules. Chirped trains of such pulse dyads can then induce a grating of the refractive index through the REMPI-seeded ionization process, radically increasing the return of probing radio waves and improving the sensitivity of stand-off impurity detection.

ACKNOWLEDGEMENTS The research described in this publication was made possible, in part, by Award No. RP2-2558 of the US Civilian Research & Development Foundation for the Independent States of the Former Soviet Union (CRDF) and, in part, by support from DARPA through Texas A&M University in association with M. Scully.

REFERENCES

1 R.M. Measures, *Laser Remote Sensing – Fundamentals and Applications* (Wiley Interscience, New York, 1984)
2 P. Rairoux, H. Schillinger, S. Niedermeier, M. Rodriguez, F. Ronneberger, R. Sauerbrey, B. Stein, D. Waite, C. Wedekind, H. Wille, L. Wöste, Appl. Phys. B **71**, 573 (2000)
3 A. Braun, G. Korn, X. Liu, D. Du, J. Squier, G. Mourou, Opt. Lett. **20**, 73 (1995)
4 E.T.J. Nibbering, P.F. Curley, G. Grillon, B.S. Prade, M.A. Franco, F. Salin, A. Mysyrowicz, Opt. Lett. **21**, 62 (1996)
5 G. Méjean, J. Kasparian, E. Salmon, J. Yu, J.-P. Wolf, R. Bourayou, R. Sauerbrey, M. Rodriguez, L. Wöste, H. Lehmann, B. Stecklum, U. Laux, J. Eislöffel, A. Scholz, A.P. Hatzes, Appl. Phys. B **77**, 357 (2003)
6 M.O. Scully, G.W. Kattawar, R.P. Lucht, T. Opatrny, H. Pilloff, A. Rebane, A.V. Sokolov, M.S. Zubairy, Proc. Natl. Acad. Sci. **99**, 10 994 (2002)
7 V. Kocharovsky, S. Cameron, K. Lehmann, R. Lucht, R. Miles, Y. Rostovtsev, W. Warren, G.R. Welch, M.O. Scully, Proc. Natl. Acad. Sci. **102**, 7806 (2005)
8 W. Kiefer (ed.), Femtosecond coherent Raman spectroscopy. Spec. Issue J. Raman Spectrosc. **31**(1–2) (2000)
9 N. Dudovich, D. Oron, Y. Silberberg, Nature **418**, 512 (2002)
10 W.S. Warren, H. Rabitz, M. Dahleh, Science **259**, 1581 (1993)

11 D.J. Tannor, S.A. Rice, J. Chem. Phys. **83**, 5013 (1985)
12 P. Brumer, M. Shapiro, Chem. Phys. **139**, 221 (1989)
13 T. Baumert, J.L. Herek, A.H. Zewail, J. Chem. Phys. **99**, 4430 (1993)
14 T. Baumert, M. Grosser, R. Thalweiser, G. Gerber, Phys. Rev. Lett. **67**, 3753 (1991)
15 T. Baumert, B. Buehler, M. Grosser, R. Thalweiser, V. Weiss, E. Wiedenmann, G. Gerber, J. Phys. Chem. **95**, 8103 (1991)
16 A. Yariv, P. Yeh, *Optical Waves in Crystals* (Wiley, New York, 1984)
17 M.N. Shneider, R.B. Miles, J. Appl. Phys. **98**, 033 301 (2005)
18 Z. Zhang, M.N. Shneider, R.B. Miles, AIAA paper no. 2006-1357 (2006)